Author Contributions:

Conceptualization: Amy X. Liu, Claire M. Zarakas, Benjamin G. Buchovecky, Linnia R. Hawkins, Alana S. Cordak, Ashley E. Cornish, Marja Haagsma, Gabriel J. Kooperman, Chris J. Still, Charles D. Koven, Alexander J. Turner, David S. Battisti, James T. Randerson, Forrest M. Hoffman, Abigail L. S. Swann
Data curation: Amy X. Liu, Claire M. Zarakas

Atmospheric Feedbacks Reverse the Sensitivity of Modeled Photosynthesis to Stomatal Function

Amy X. Liu[1] [ID], **Claire M. Zarakas[1]** [ID], **Benjamin G. Buchovecky[1]** [ID], **Linnia R. Hawkins[2]** [ID], **Alana S. Cordak[3]** [ID], **Ashley E. Cornish[3]** [ID], **Marja Haagsma[4]** [ID], **Gabriel J. Kooperman[3]** [ID], **Chris J. Still[5]** [ID], **Charles D. Koven[6]** [ID], **Alexander J. Turner[1]** [ID], **David S. Battisti[1]** [ID], **James T. Randerson[7]** [ID], **Forrest M. Hoffman[8]** [ID], and **Abigail L. S. Swann[1,9]** [ID]

[1]Department of Atmospheric and Climate Science, University of Washington, Seattle, WA, USA, [2]Department of Earth and Environmental Engineering, Columbia University, New York, NY, USA, [3]Department of Geography, University of Georgia, Athens, GA, USA, [4]Department of Biological and Ecological Engineering, Oregon State University, Corvallis, OR, USA, [5]Department of Forest Ecosystems and Society, Oregon State University, Corvallis, OR, USA, [6]Lawrence Berkeley National Laboratory, Climate and Ecosystem Sciences Division, Berkeley, CA, USA, [7]Department of Earth System Science, University of California, Irvine, Irvine, CA, USA, [8]Oak Ridge National Laboratory, Oak Ridge, TN, USA, [9]Department of Biology, University of Washington, Seattle, WA, USA

Abstract Stomata mediate fluxes of carbon and water between terrestrial plants and the atmosphere. These fluxes are governed by stomatal function and can be modulated in many Earth system models by an empirical parameter within the calculation of stomatal conductance, the stomatal slope (g_{1M}). Intuitively, g_{1M} represents the marginal water cost of carbon, relating it to the emergent plant property of water use efficiency. Observations show that g_{1M} can range widely across and within plant types in varying environments, and this distribution of g_{1M} is not captured within Earth system models which represent each plant type with a single g_{1M} value. Here we examine how g_{1M} influences photosynthesis using coupled Earth system model simulations by perturbing g_{1M} to observed 5th and 95th percentiles for each plant type. We find that high g_{1M} reduces photosynthesis nearly everywhere, while low g_{1M} has regionally dependent responses. Under fixed atmospheric conditions, low g_{1M} increases photosynthesis in the Amazon and central North America but decreases photosynthesis in boreal Canada. These responses reverse when the atmosphere responds interactively due to spatially differing sensitivity to increases in temperature and vapor pressure deficit. Choice of g_{1M} also influences photosynthetic response to changes in atmospheric carbon dioxide (CO_2), with lower and higher g_{1M} modifying total global response to elevated 2x preindustrial CO_2 by +6.4% and −9.6%, respectively. Our work demonstrates that atmospheric feedbacks are critical for determining the photosynthetic response to g_{1M} assumptions and some regions are particularly sensitive to choice of g_{1M}.

Plain Language Summary Plants affect the Earth system's carbon, water, and energy fluxes through photosynthesis and transpiration, regulated by stomata that control gas exchange. Stomatal function controls the water cost per carbon gain for photosynthesis, where lower water cost means less water lost per carbon gain and higher water cost means more water lost. Observations show a range of stomatal function across and within plant types in varying environments which are not captured in Earth system models. In our study, we explored how changes in stomatal function impact photosynthesis using an Earth system model. We find higher water cost generally decreases photosynthesis everywhere while lower water cost has mixed effects, increasing photosynthesis in the Amazon and central North America but decreasing it in boreal Canada. These responses change when we allow the atmosphere to respond to changes on land, mainly due to spatially varying sensitivity to warmer temperature and drier air. Additionally, changes in stomatal function alter photosynthetic response to higher atmospheric carbon dioxide concentrations, with lower and higher water cost changing global photosynthesis by +6.4% and −9.6%, respectively. Our study demonstrates that accounting for atmospheric responses to land changes is critical for understanding the sensitivity of photosynthesis to stomatal function.

1. Introduction

Stomatal functioning mediates water loss through transpiration and carbon gain through photosynthesis, influencing the water and carbon fluxes between plants and the atmosphere (G. B. Bonan, 2008). A change in stomatal function shifts how stomata physiologically regulates the gas exchange, altering conductance of atmospheric carbon dioxide (CO_2) for photosynthesis and water vapor for transpiration.

Formal analysis: Amy X. Liu
Funding acquisition: Gabriel J. Kooperman, Chris J. Still, Charles D. Koven, James T. Randerson, Forrest M. Hoffman, Abigail L. S. Swann
Investigation: Amy X. Liu, Claire M. Zarakas, Abigail L. S. Swann
Methodology: Amy X. Liu, Claire M. Zarakas, Chris J. Still, Abigail L. S. Swann
Project administration: Abigail L. S. Swann
Resources: Abigail L. S. Swann
Software: Amy X. Liu, Claire M. Zarakas
Supervision: Abigail L. S. Swann
Validation: Amy X. Liu
Visualization: Amy X. Liu
Writing – original draft: Amy X. Liu
Writing – review & editing: Amy X. Liu, Claire M. Zarakas, Benjamin G. Buchovecky, Linnia R. Hawkins, Alana S. Cordak, Ashley E. Cornish, Marja Haagsma, Gabriel J. Kooperman, Chris J. Still, Charles D. Koven, Alexander J. Turner, David S. Battisti, James T. Randerson, Abigail L. S. Swann

The theory for optimal stomatal behavior suggests that plants dynamically adjust their stomatal opening (and thus conductance) to achieve a balance between the rate of photosynthesis and water loss from transpiration, resulting in an "optimal" relationship that can be expressed mathematically (Arneth et al., 2002; Cowan & Farquhar, 1977). Empirical formulations for stomatal conductance are derived using observations of stomatal behavior under different environmental conditions including atmospheric dryness, temperature, and atmospheric CO_2 concentration (Ball et al., 1987; Leuning, 1995). Medlyn et al. (2011) developed a unified formulation for stomatal conductance, based off the optimal theory and expressed in empirical form, yielding physiologically meaningful parameters that can be estimated from data. Regardless of the approach taken to represent stomatal behavior under different environmental conditions, more open stomata tend to increase both transpiration and the uptake of carbon for photosynthesis, and vice-versa for more closed stomata. As a result, stomatal conductance, photosynthesis and transpiration are tightly coupled under most conditions, though they can become decoupled under high temperature conditions (De Kauwe et al., 2019). Stomatal function governs the ratio of these processes, or the marginal water cost of carbon gain.

1.1. Uncertainty in g_{1M}

In common process-based models that explicitly represent photosynthesis rates and stomatal conductance (e.g., Ball et al., 1987; Farquhar et al., 1980; Leuning, 1995; Medlyn et al., 2011), stomatal function can be modified by one of the empirically fit parameters. We will focus here on the Medlyn et al. (2011) formulation of stomatal conductance, g_s, given by

$$g_s = g_0 + 1.6\left(1 + \frac{g_{1M}}{\sqrt{VPD}}\right)\frac{A_n}{c_s}, \qquad (1)$$

where A_n is photosynthesis, c_s is the atmospheric CO_2 concentration, VPD is vapor pressure deficit, and g_0 is the Medlyn intercept (minimum stomatal conductance, when the stomata are completely closed). A_n is coupled to g_s, and an increase in stomatal conductance relates to an increase in photosynthesis. The stomatal slope, g_{1M}, is an empirically estimated parameter that is determined by the marginal water cost of carbon gain and related to the emergent plant property of intrinsic water use efficiency (iWUE; Medlyn et al., 2011).

Observationally based estimates of g_{1M} exist for only a small subset of climatic space represented on Earth. Even in this limited climate space, g_{1M} shows a large variation both across plant types and within a plant type (Lin, Medlyn, Duursma, et al., 2015; Y. Liu et al., 2021; Wolz et al., 2017). However, in many land surface models, including those within Earth system models, for tractability a single g_{1M} value is assigned to each plant type, even though the plant type may exist in many locations with different climates. In the land surface component of the Community Earth System Model version 2 (CESM2), the average g_{1M} within a grid cell has variation (Figure 1a) since there are 14 different plant functional types (PFTs), and each PFT has its own distribution and a different g_{1M} derived from Lin, Medlyn, Duursma, et al. (2015). Given that there is a large observed range in the value of g_{1M} for each plant type (e.g., Lin, Medlyn, Duursma, et al., 2015), the actual distribution of average g_{1M}, and thus stomatal function, is also uncertain.

Photosynthesis is expected to increase while g_s is expected to decrease in response to elevated atmospheric CO_2 (Adams et al., 2020; Li et al., 2023). Under elevated CO_2, CO_2 diffuses more easily into leaves, prompting plants to alter their stomatal functioning to optimize carbon gain to water loss, which could lead to either further increases in photosynthesis or reductions in transpiration per leaf area (Frank et al., 2015; Keenan et al., 2013). Additionally, more photosynthesis can lead to increases in leaf area, which could increase total photosynthesis and transpiration (Field et al., 1995).

To evaluate the role of stomatal functioning, we investigate the sensitivity of photosynthesis to different assumptions about g_{1M} in an Earth system model under both historical and future climate conditions. Intuitively, low g_{1M} corresponds to less water loss per unit carbon gain (low water cost) and high g_{1M} corresponds to more water loss per carbon gain (high water cost). We examine two research questions: first, what are the mechanisms and feedbacks through which different assumptions about g_{1M} impact photosynthesis and how do they vary spatially (Section 3.2); and second, what is the impact of uncertainty in g_{1M} on the response of photosynthesis to elevated
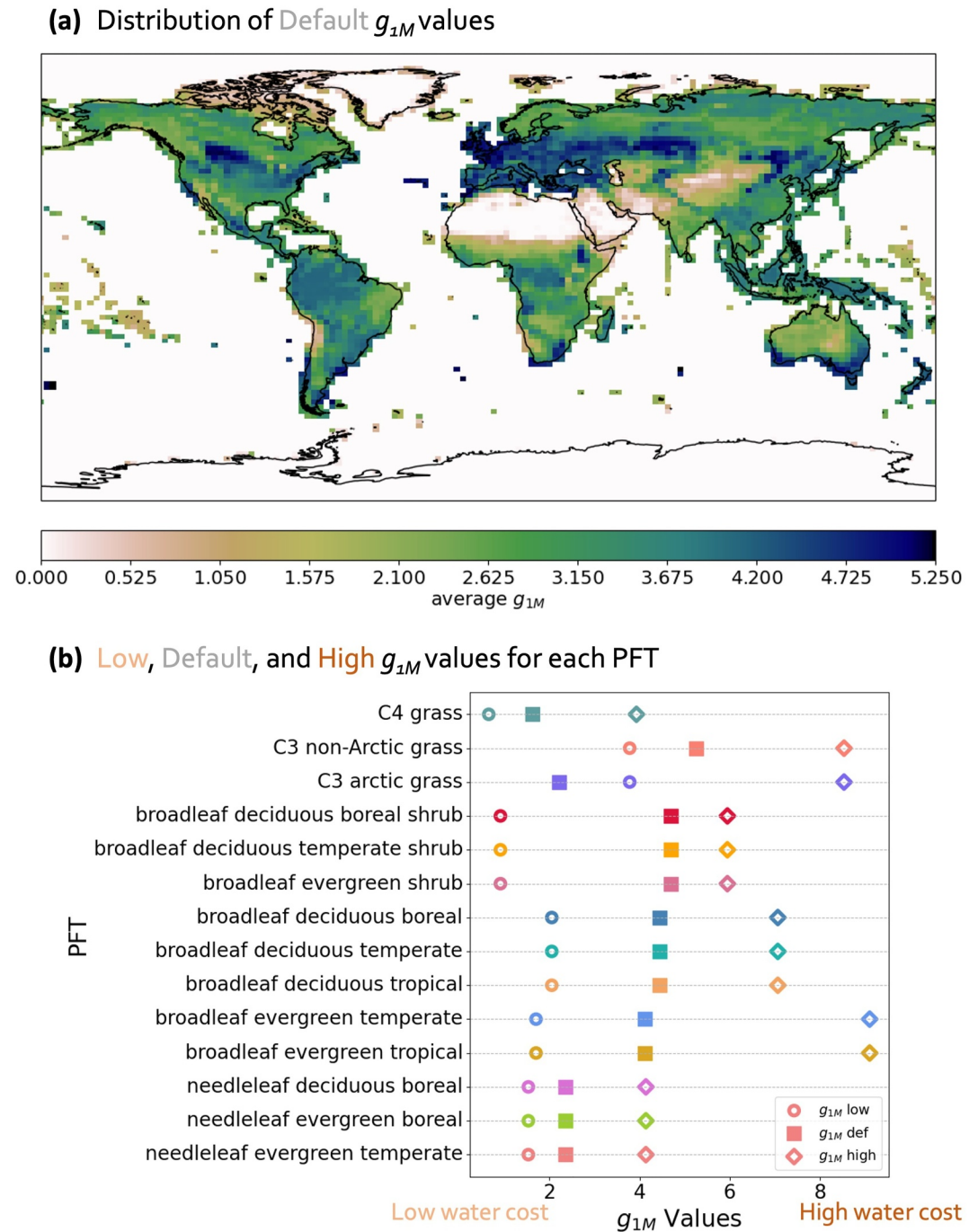
Figure 1. (a) Spatial plot of default PFT-area-weighted g_{1M} values used in CLM5. (b) Plot of the default and perturbed stomatal slope parameter, g_{1M}, for each vegetation type in the CLM5.

atmospheric CO_2 concentrations (Section 3.3)? We focus our analysis on the response of photosynthesis as it integrates the response of both carbon and water cycling to assumptions about stomatal function, with g_{1M} serving as a metric to quantify these variations.

2. Methods

2.1. Model Configurations

We used the Community Earth System Model version 2 (CESM2; Danabasoglu et al., 2020), an open-source Earth system model, to estimate the response of photosynthesis to different assumptions of g_{1M}. CESM2 is comprised of the Community Land Model 5 (CLM5; D. M. Lawrence et al., 2019), the Community Atmosphere Model 6 (CAM6; Bogenschutz et al., 2018), and a slab ocean based on output from the CESM2 Coupled Model Intercomparison Project Phase 6 (CMIP6) preindustrial control run (Danabasoglu & Gent, 2009). We performed global-scale simulations of CESM2 at $0.9 \times 1.25°$ spatial resolution.

In order to isolate the impacts of atmospheric response and dynamic leaf area to different values of g_{1M}, we defined two configurations of CESM2. The "Land-Atmosphere" configuration (LndAtm) was run with a dynamic atmosphere and a land model that included active biogeochemistry and prognostic leaf area that allowed for leaf area to dynamically respond to climate, resulting in changes in both atmospheric conditions and leaf area in response to g_{1M} (water cost) perturbations. The active biogeochemistry component tracks both carbon and nitrogen using vertically resolved carbon pools and representation of nitrogen cycling (D. M. Lawrence et al., 2019). The "Land-Only-Fixed-Leaf" configuration (LndOnly) is the same land model but with the leaf area phenology specified as a repeating seasonal cycle of climatological leaf area, so there were no changes in both atmospheric conditions and year-to-year leaf area in response to g_{1M} perturbations. The Land-Only-Fixed-Leaf simulations are used as a counterfactual to understand the changes in stomatal function, photosynthesis, and climate in the Land-Atmosphere preindustrial CO_2 simulations.

In order to compare the response of atmospheric feedbacks and prognostic leaf area under equivalent meteorological conditions, we prescribed the meteorological forcing in the Land-Only-Fixed-Leaf simulations using the output of the default g_{1M} Land-Atmosphere simulation saved at 3 hourly intervals. The 3-hourly meteorological data is interpolated to 30 min time resolution to drive the Land-Only-Fixed-Leaf simulations. We analyzed the last 80 years of a 120-year simulation, after discarding the first 40 years to allow the system to reach equilibrium.

Broadly in CLM5, g_s and photosynthesis are calculated iteratively from environmental conditions estimated at the leaf level, including air temperature, vapor pressure deficit (VPD), atmospheric CO_2 concentration, and photon flux density using g_s formulated as in Medlyn et al. (2011) (Equation 1), and photosynthesis from Farquhar et al. (1980), G. J. Collatz et al. (1991), and G. Collatz et al. (1992). Total canopy latent heat fluxes are altered by g_s, leaf area, leaf boundary layers and aerodynamic resistance. More details can be found in the CLM5 technical note in Section 2.5.3 and 2.9 (D. Lawrence et al., 2018).

CLM5 with default parameters represents photosynthesis well relative to other land models in the International Land Model Benchmarking (ILAMB) in an integrated assessment (e.g., biases, spatial patterns, etc.) against observational data sets, and its global photosynthesis (119 PgC/year) is similar to that of FLUXNET-MTE (118 PgC/year) (D. M. Lawrence et al., 2019). Regionally, CLM5 captures the spatial and seasonal patterns of photosynthesis in contiguous United States when compared to FLUXNET-MTE, though photosynthesis is underestimated during the growing season (Cheng et al., 2021). These assessments mainly focus on simulations with prescribed atmospheric forcing, but CESM2 simulations with atmospheric feedbacks also perform relatively well for photosynthesis against other Earth system models (D. M. Lawrence et al., 2019).

2.2. g_{1M} Perturbations

We investigate the response of photosynthesis to assumptions about plant stomatal function by perturbing the stomatal slope parameter, g_{1M}, within Equation 1. These perturbations reflect variations in stomatal function, as g_{1M} is related to the marginal water cost of carbon (Medlyn et al., 2011). To add intuition, we additionally describe our results in terms of the change in water cost associated with a perturbed g_{1M}, where high g_{1M} represents a higher cost of water and vice versa. This intuition is consistent with measurements of g_{1M} across FLUXNET stations, where drier stations tend to show lower g_{1M} and more water use efficient behavior while stations in wetter regions tend to show higher g_{1M} and less water use efficient behavior (De Kauwe et al., 2015; Knauer et al., 2015; Lin, Medlyn, Duursma, et al., 2015). We perturbed g_{1M} to a minimum and maximum for each PFT based on the 5th and 95th percentile from observations (Lin, Medlyn, Duursma, et al., 2015; Figure 1b), such that we have one set of simulations that use the 5th percentile values for g_{1M} ("low g_{1M}" or "low water cost") and one set of simulations that use 95th percentile values for g_{1M} ("high g_{1M}" or "high water cost"). The range of g_{1M} across PFTS from the

Table 1
Summary of Simulations

Group	Simulation name	CO_2	Atmosphere	Leaf area	g_{1M} (water cost)
LndAtm	Land-Atmosphere low g_{1M}	$1 \times CO_2$	dynamic	prognostic	low
	Land-Atmosphere default g_{1M}				default
	Land-Atmosphere high g_{1M}				high
LndOnly	Land-Only-Fixed-Leaf low g_{1M}	$1 \times CO_2$	prescribed	prescribed	low
	Land-Only-Fixed-Leaf default g_{1M}				default
	Land-Only-Fixed-Leaf high g_{1M}				high
LndAtm2x	Land-Atmosphere $2 \times CO_2$ low g_{1M}	$2 \times CO_2$	dynamic	prognostic	low
	Land-Atmosphere $2 \times CO_2$ default g_{1M}				default
	Land-Atmosphere $2 \times CO_2$ high g_{1M}				high

Note. The sensitivity to g_{1M} is calculated by comparing simulations within an experiment group (e.g., LndAtm low g_{1M} minus LndAtm default g_{1M}; Section 2.3.1). The effect of atmospheric and leaf area feedbacks is calculated by comparing experiment groups LndAtm and LndOnly (Section 2.3.2). The total response to elevated CO_2 is calculated by taking experiment group LndAtm2x minus group LndAtm (Section 2.3.3).

leaf-level estimates used in our study is similar to the range derived from isotopic measurements and FLUXNET observations (Medlyn et al., 2017).

We quantify the effect of a change in g_{1M} by comparing the low or high g_{1M} simulations against simulations with the default g_{1M} parameter values used in CLM5, noting that these default values do not represent the mean or median of the range of observations we used for perturbation (Figure 1b). The average g_{1M} for any given grid cell is a weighted average that varies due to the distribution of PFTs within the grid cell and the range of default g_{1M} values across PFTs (Figure 1a).

2.3. Simulation Design

In order to isolate the effects of multiple processes that comprise the full climate and ecosystem response to stomatal function, we performed nine simulations (Table 1). For each simulation we set g_{1M} (water cost) to either default, low, or high values which intuitively corresponds to default, low, or high water cost per carbon gain. We tested two configurations of CESM2, one with atmosphere and prognostic leaf area components working interactively ("Land-Atmosphere"; experimental group "LndAtm" in Table 1), and one where both meteorological forcing and leaf area phenology are prescribed ("Land-Only-Fixed-Leaf"; experimental group "LndOnly" in Table 1). Both configurations were run at preindustrial atmospheric CO_2 concentrations (284.7 ppm) and the Land-Atmosphere configuration was additionally run with 2x preindustrial atmospheric CO_2 concentrations (569.4 ppm; experimental group "LndAtm2x" in Table 1) in order to assess the sensitivity of climate and photosynthesis to uncertainty in g_{1M} under elevated CO_2 concentrations. Going forward, we refer to simulations by their experimental group names (e.g., LndAtm, LndOnly, and LndAtm2x) for readability in the text, while figures and tables use the full simulation name (e.g., Land-Atmosphere low g_{1M} and Land-Only-Fixed-Leaf low g_{1M}).

2.3.1. Quantifying Impact of Perturbations in g_{1M}

We implement perturbations to the g_{1M} parameter as described above, resulting in simulations with lower or higher g_{1M} (water cost) relative to the default in CLM5. To quantify a photosynthesis or climate response to a change in g_{1M}, we calculated the response of a variable by comparing the simulations with either low or high g_{1M} against the simulations with default g_{1M} (comparison within an experiment group in Table 1). We averaged across all 80 post-spinup years to quantify the equilibrium response to a g_{1M} perturbation. We report both the actual difference between simulations and percentage difference between simulations for individual variables. Unless otherwise noted, percentage difference for a variable was calculated by taking the relative difference of that variable between two simulations and dividing it by the time average in the default g_{1M} simulation. The focus of our analysis is on annual photosynthesis. Generally, the response of annually averaged photosynthetic is similar to that averaged over from the growing season only, and so we report the annual averages here.

2.3.2. Quantifying Impact of Dynamic Atmosphere and Prognostic Leaf Area

To understand how the combined atmospheric and leaf area feedbacks modify the climate impact of g_{1M} (water cost), we compared the response of a variable to a g_{1M} perturbation between experimental groups LndAtm and LndOnly (Table 1). For example, we compared the difference between the low and default g_{1M} simulations within LndOnly with the difference between the low and default g_{1M} simulations within LndAtm. In addition to calculating the absolute difference we also compared just the change in sign of photosynthetic response by filtering for grid cells with a sign change in photosynthetic response to g_{1M} perturbation between LndOnly and LndAtm.

2.3.3. Quantifying Impact of Elevated Atmospheric CO_2

We performed two comparisons with the $2xCO_2$ simulations. First, we quantified the absolute response of a variable to an increase in atmospheric CO_2 by comparing $2xCO_2$ simulations to their parallel configuration $1xCO_2$ simulations, for example, LndAtm2x low g_{1M} − LndAtm low g_{1M} (Table 1). Second, we quantified how the response of a variable to elevated CO_2 changes with g_{1M}. We did this by comparing the response to elevated CO_2 across different g_{1M} values, for example (LndAtm2x low g_{1M} − LndAtm g_{1M}) − (LndAtm2x default g_{1M} − LndAtm g_{1M}), which allowed us to remove the effect of elevated CO_2 and look at how changes in g_{1M} modify the response.

2.3.4. Regional Analysis

In addition to global climate response to perturbations in g_{1M} (water cost), we focused on the response in three regions, each spanning different background climates: the tropical forest Amazon (13°S to 5°S and 68°W to 57°W), the temperate grassland central North America (central NA; 40°N to 52°N and 103°W to 96°W), and boreal forest Canada (50°N to 57°N and 78°W to 69°W). We calculated the regional climate response by taking the area-weighted average across all of the grid cells in each region.

2.4. Perturbed Meteorology Simulations

In addition to comparing our different g_{1M} (water cost) simulations, we used an additional set of simulations to directly isolate the effects of temperature and vapor pressure deficit (VPD) on photosynthesis and aid in the interpretation of our results from the perturbed g_{1M} simulations. These are sensitivity experiments, intended to isolate the effect of individual climate factors. We refer to these simulations as "perturbed meteorology" simulations. In each simulation, a single meteorological variable was modified in a version of the model with a prescribed atmosphere and prognostic leaf area at default g_{1M} configuration. We completed two perturbed meteorology simulations. The first isolates the effects of temperature by increasing the bottom-of-atmosphere temperature in each grid cell by 1°C, while keeping the specific humidity constant. VPD is calculated based on the bottom-of-atmosphere temperature, pressure, and specific humidity, so it is an indirect effect of temperature. Thus the temperature perturbed simulation accounts for both the indirect and direct effects of temperature on photosynthesis. The second simulation isolated the effects of VPD by imposing a 10% increase in the bottom-of-atmosphere specific humidity in each grid cell, while keeping the temperature constant. This allows us to isolate the effects of VPD on photosynthesis that are not driven by changes in temperature. Details on how we calculated the expected response of photosynthesis to temperature and VPD changes from g_{1M} perturbations can be found in Text S1 in Supporting Information S1.

2.5. Statistical Significance

We used a test of statistical significance to determine if annually averaged responses in the perturbed g_{1M} (water cost) simulations differed from those in the default g_{1M} simulation. We report our results as statistically significant when a two-tailed student's t-test with an assumed 40 degrees of freedom has a p-value that passes the false discovery rate of 0.05. We use a conservative estimate for degrees of freedom that assumes variables exhibit an auto-correlation of less than 2 years. The false discovery rate, or the fraction of false positives, is important in our analysis because we perform a t-test at many grid cells and accounting for it makes our p-values more conservative (Wilks, 2016). In the spatial maps, grid cells that do not pass the statistical test are indicated with stippling.
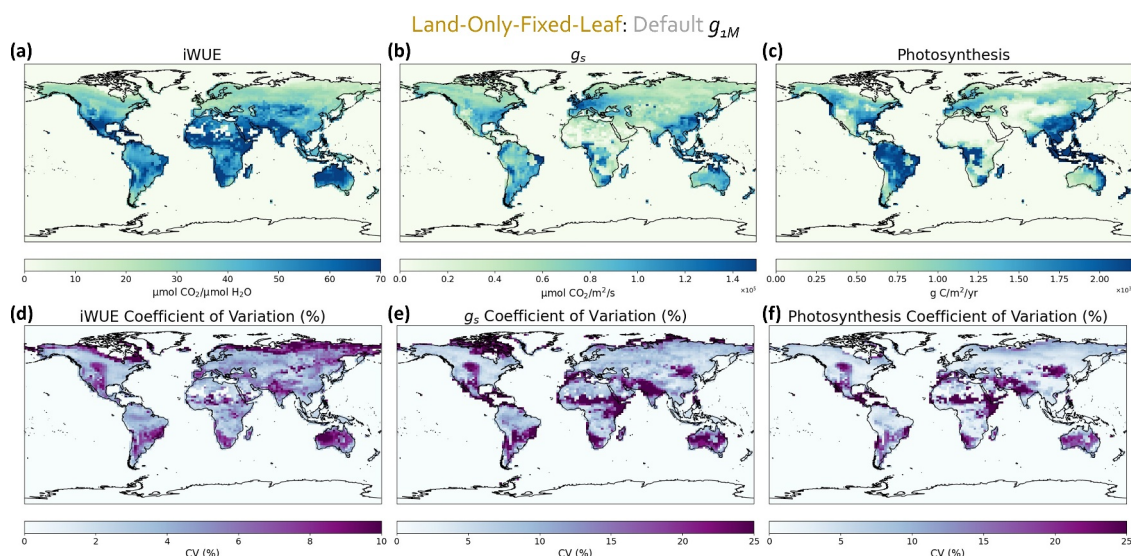
Figure 2. Spatial plots of Land-Only-Fixed-Leaf (LndOnly) default g_{1M} (water cost) simulations showing the mean of (a) iWUE, (b) g_s, and (c) photosynthesis. (d–f) Show the corresponding coefficient of variation (standard deviation divided by the mean) for iWUE, g_s, and photosynthesis.

For simple comparisons between two simulations (e.g., LndAtm low g_{1M} − LndAtm default g_{1M}), we compare their output distributions with the null hypothesis that there is no statistical difference between them. For comparisons of responses between simulations (e.g., (LndAtm low g_{1M} − LndAtm g_{1M}) and (LndOnly low g_{1M} − LndOnly default g_{1M})), we use bootstrapping ($n = 1,000$) to generate empirical distributions of the responses and test for significance. Since simulation years are samples of a climate-state rather than aligned in time, we assess statistical significance through bootstrapped distributions rather than direct year-to-year comparison.

3. Results

3.1. Intrinsic Water Use Efficiency at Default g_{1M}

Plant intrinsic water use efficiency (iWUE) is the ratio of the rate of carbon gain to the rate of water loss; it is an emergent property that results from the coupled behavior of photosynthesis and g_s. In the LndOnly default g_{1M} simulation, the most simple simulation with no atmospheric and leaf area feedbacks, iWUE has a global mean of 41.29 μmolCO$_2$/μmolH$_2$O, g_s has a global mean of just under 60,000 μmolCO$_2$/m^2/s, and photosynthesis has a global mean of 853.41 gC/m^2/year. Spatially, iWUE is higher in lower latitudes, g_s is higher in regions such as South America, Central and Eastern North America, Europe, Eastern China, Southeast Asia, and Australia, while photosynthesis tends to be higher in the tropics (cf. Figures 2a–2c). All three share a similar spatial pattern of coefficient of variation (the magnitude of the standard deviation relative to the mean; cf. Figures 2d–2f), which is expected given their coupled relationship.

In the LndOnly simulations, a high g_{1M} perturbation increases the global average g_s, or diffusion of CO$_2$ into leaf, by around 41,700 μmolCO$_2$/m^2/s (+70.3%) from default g_{1M} and low g_{1M} perturbation decreases global average g_s by just over 20,000 μmolCO$_2$/m^2/s (−33.9%). The inclusion of atmospheric and leaf area feedbacks in the LndAtm simulations yields a similar magnitude of g_s response and an amplified iWUE response compared to those in the LndOnly simulations (cf. Figures S1–S4a and S4b in Supporting Information S1). This suggests that changes in iWUE are mainly driven by changes in photosynthesis.

3.2. Photosynthetic Response to g_{1M}

Total global photosynthesis in the LndAtm simulations varied across our g_{1M} (water cost) perturbations, with 120 PgC/year in the default g_{1M}, 99 PgC/year in the high g_{1M}, and 112 PgC/year in the low g_{1M}. Below we describe the causes for changes in photosynthesis associated with each g_{1M} perturbation in more detail.
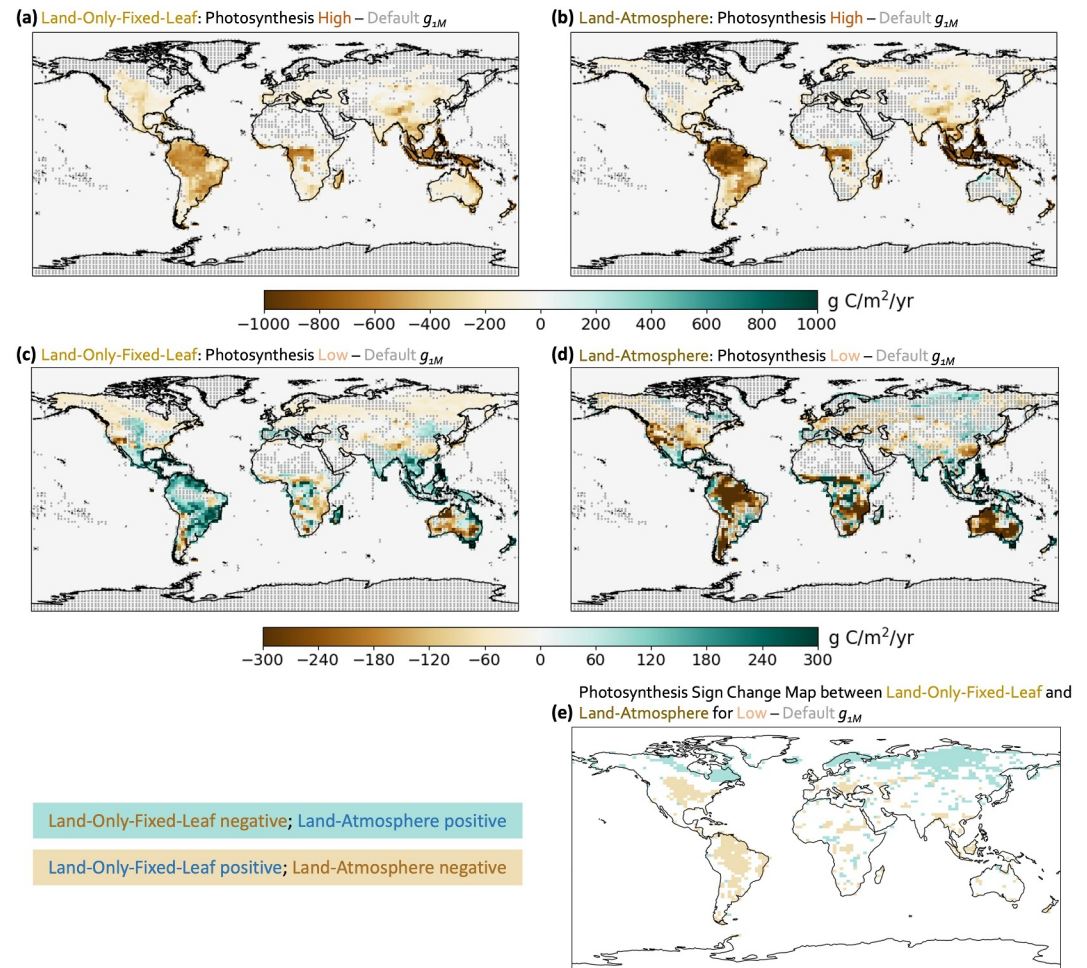
Figure 3. Spatial difference plots of photosynthesis for high minus default g_{1M} (water cost) at (a) Land-Only-Fixed-Leaf (LndOnly) and (b) Land-Atmosphere (LndAtm) configurations and low minus default g_{1M} (water cost) at (c) Land-Only-Fixed-Leaf (LndOnly) and (d) Land-Atmosphere (LndAtm) configurations. The response to higher and lower g_{1M} are at different scales. Stippled grid cells represent differences that are not statistically significant. Statistical methods are detailed in Section 2.5. (e) A spatial plot showing the difference in the sign of the photosynthetic change in the Land-Only-Fixed-Leaf (LndOnly) and Land-Atmosphere (LndAtm) low minus default g_{1M} simulations. Colored grids indicate where the sign of the change in the Land-Atmosphere (LndAtm) simulation is opposite to that in the Land-Only-Fixed-Leaf (LndOnly) simulation and the color represents the direction of change.

3.2.1. Impacts of High g_{1M}

In the LndAtm high g_{1M} (high water cost) simulation, photosynthesis decreased across the globe (Figure 3b) relative to the default g_{1M} simulation by 138 gC/m^2/year. There were larger absolute decreases in photosynthesis near the equator, due to greater overall plant productivity in the tropics. Modeled photosynthesis decreased with higher g_{1M} because plants open their stomata and transpire more (Figures S2b and S2c in Supporting Information S1) leading to a cascade of changes to other variables that affect photosynthesis. Greater transpiration rates deplete plant and soil water supply making plants more soil water stressed (Figure S2d in Supporting Information S1), leading to a decrease in the number of leaves that a plant can support (Figure S2g in Supporting Information S1) which decreased total photosynthesis (Figure 3b). VPD decreased along with decreases in surface temperature due to greater transpiration, which decreased atmospheric water stress. One might have expected the decrease in VPD to alleviate overall plant water stress, however the increase in soil water stress was greater than the decrease in atmospheric water stress with higher g_{1M} which accounts for the decrease in photosynthesis in our simulations.

The photosynthetic response to higher g_{1M} was similar with and without dynamic atmosphere and prognostic leaf area (cf. Figures 3a and 3b). Both configurations showed decreases in photosynthesis across the globe in response to higher g_{1M} with similar spatial patterns but with a larger magnitude of change in the LndAtm high g_{1M} simulation driven largely by leaf area decreases (Figure S2g in Supporting Information S1) that are precluded in the LndOnly high g_{1M} simulation.

3.2.2. Impacts of Low g_{1M}

Given that higher water cost led to lower photosynthesis due to soil water stress, our naive expectation is that lower water cost should lead to higher rates of photosynthesis. However, the photosynthetic response in LndAtm to lowered g_{1M} (lowered water cost) is generally negative (although much smaller in magnitude than the response to higher g_{1M} perturbations; cf. Figures 3b and 3d, with a global average photosynthesis decrease of 50 gC/m^2/year for lower g_{1M}. There were large regions in which photosynthesis rates increased in the lower g_{1M} compared to the default g_{1M} experiment (e.g., over southeast Asia and the Sahel; Figure 3d). The spatial pattern of change in photosynthesis due to lower g_{1M} is similar to the change in precipitation, suggesting a connection between the two (cf. Figure 3d and Figure S4h in Supporting Information S1). However, water availability variables such as soil water stress and VPD do not share the same response pattern as photosynthesis (cf. Figure 3d and Figures S4f and S4g in Supporting Information S1). Interestingly, the precipitation response pattern to low g_{1M} is also similar to that in response to higher CO_2 reported in Kooperman et al. (2018), which is consistent since plant water cost per carbon gain generally decreases with higher CO_2.

In contrast to the high g_{1M} simulations, the photosynthetic response to lower g_{1M} is sensitive to land-atmosphere and dynamic vegetation feedbacks (cf. Figures 3c and 3d), with some regions showing a response in opposite directions. Regions with the same direction of photosynthetic response between the LndOnly and LndAtm low g_{1M} simulations tend to have a greater response in the LndAtm simulation (cf. Figures 3c and 4d; Figure S4g in Supporting Information S1). In several regions, the sign of response of photosynthesis to low g_{1M} depends on whether the atmosphere and/or leaf area are allowed to change including in the Amazon, central North America (central NA), and boreal Canada (Figure 3e). We discuss each of these three regions in further detail below.

3.2.3. Regional Responses to Low g_{1M}

We examine how the regional response of photosynthesis to g_{1M} (water cost) differs between LndAtm and LndOnly in three focal regions; the Amazon, central NA, and boreal Canada.

In the Amazon, in response to lower g_{1M} (lower water cost), photosynthesis decreased in LndAtm but increased in LndOnly (cf. Figures 3c and 3d; Table 2; Figure 4a), indicating that conditions controlling photosynthesis are greatly affected by atmosphere and/or dynamic vegetation feedbacks. Transpiration in the Amazon decreased in both configurations as plants closed their stomata in response to lower g_{1M}. Temperature and VPD both increase when the atmosphere is allowed to dynamically respond in LndAtm, while in LndOnly the meteorological conditions are identical between all experiments, and thus there are no changes in temperature and VPD.

Decreases in transpiration cause increases in temperature (and an increase in VPD) and a reduction in clouds further increases temperature and VPD in the Amazon (Table 2). Under decreased evaporation, in this case transpiration, the warming effect of decreased cloud cover is typically larger than decreased latent cooling (Laguë et al., 2023). As in the case of the Amazon, central NA shows a decrease in photosynthesis with lower g_{1M} in LndAtm and an increase in LndOnly (Table 2; Figure 4c). We also found warming due to decreased latent cooling central NA, and shortwave cloud feedbacks occurred in all three of our focal regions. The Amazon had the largest magnitude of temperature increase (2.72°C) compared to central NA (0.97°C) and boreal Canada (0.59°C), and we note that this temperature increase in the Amazon occurred on top of an already higher baseline temperature.

Over boreal Canada, photosynthesis increased in response to lower g_{1M} in LndAtm and decreased in LndOnly (opposite to the Amazon and central NA; Table 2; Figure 4e). As in the other regions, the LndAtm low g_{1M} simulation had much greater increases in surface temperature and in VPD (Table 2) relative to the simulations with prescribed atmospheric conditions. The VPD increase in boreal Canada was smaller than in the Amazon, consistent with a smaller absolute temperature change (cf. Figures 4a and 4e; Table 2).

We attribute the cause of the response of photosynthesis to temperature and VPD using our perturbed meteorology simulations. In both the Amazon and central NA we find an increase in temperature alone tended to slightly
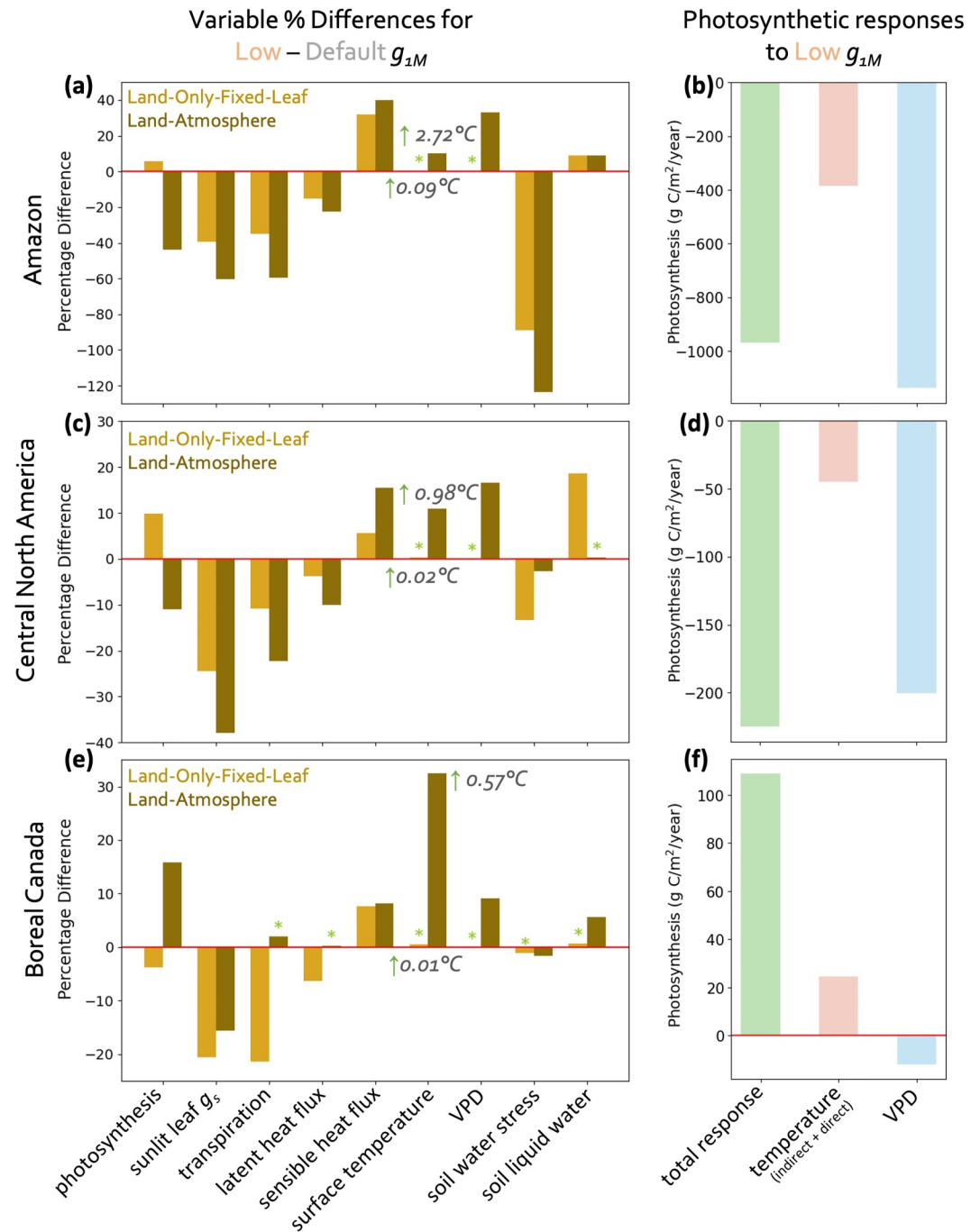
Figure 4. Percentage differences of photosynthesis and variables that can influence photosynthesis between the low and default g_{1M} (water cost) simulations using the Land-Only-Fixed-Leaf (LndOnly) and Land-Atmosphere (LndAtm) configurations in the (a) Amazon, (c) central North America, and (e) boreal Canada. Bars with a green (*) are not statistically different from zero. Statistical methods are detailed in Section 2.5. The expected photosynthetic response estimated from perturbed meteorology for temperature ($\frac{\Delta GPP_T}{\Delta T_T}\delta T_{LndAtm}$; red bar) and VPD ($\frac{\Delta GPP_{VPD}}{\Delta VPD_{VPD}}\delta VPD_{LndAtm}$; blue bar) in (b) the Amazon, (d) central NA, and (f) boreal Canada. Temperature includes both direct effects of warming and indirect effects of VPD. The absolute difference in photosynthesis due to the change in g_{1M} (low minus default) between the Land-Atmosphere (LndAtm) and Land-Only-Fixed-Leaf (LndOnly) configurations are shown in green ($\Delta GPP_{LndAtm} - \Delta GPP_{LndOnly}$). Note that the y-axis is unique to each plot.

Table 2
Climate Variable Responses to Low g_{1M} (Low Minus Default g_{1M})

	Amazon				Central NA				Boreal Canada			
	Land-only-fixed-leaf		Land-atmosphere		Land-only-fixed-leaf		Land-atmosphere		Land-only-fixed-leaf		Land-atmosphere	
Variable	unit	%	unit	%	unit	%	unit	%	unit	%	unit	%
Photosynthesis (gC/m^2/yr)	**110***	**5.7***	**−859***	**−43.9***	**109***	**9.8***	**−116***	**−11.0***	**−22.6***	**−3.8***	**86.2***	**15.8***
Sunlit leaf g_s (gH$_2$O/m^2/s)	−0.77*	−39.5*	−1.12*	−60.2*	−0.55*	−24.5*	−0.78*	−37.9*	−0.36*	−20.6*	−0.28*	−15.7*
Transpiration (W/m^2)	−20.7*	−35.1*	−35.7*	−59.5*	−3.53*	−10.8*	−6.66*	−22.3*	−1.84*	−21.3*	0.15	2.1
Latent heat flux (W/m^2)	−14.4*	−15.1*	−21.6*	−22.4*	−1.86*	−3.7*	−4.81*	−10.1*	−1.56*	−6.3*	−0.05	−0.2
Sensible heat flux (W/m^2)	13.2*	31.8*	16.2*	39.8*	1.60*	5.6*	4.44*	15.5*	1.42*	7.6*	1.58*	8.2*
Soil water stress (unitless)	−0.40*	−89.1*	−0.49*	−124*	−0.11*	−13.3*	−0.03*	−2.7*	−0.01	−1.0	−0.01*	−1.6*
Soil liquid water (kg)	80.5*	+8.8*	81.6*	9.0*	123*	18.7*	2.73	0.4	4.48	0.6	40.4*	5.6*
Surface temperature (°C)	0.09	0.3	2.72*	10.2*	0.02	0.3	0.98*	11.0*	0.01	0.5	0.57*	32.5*
VPD (Pa)	-	-	674*	+33.0*	-	-	127*	16.6*	-	-	28.0*	9.1*
Low cloud cover (fraction)	-	-	−0.07*	−39.9*	-	-	−0.04*	−15.3*	-	-	−0.02*	−3.7*
Incident solar radiation (W/m^2)	-	-	2.00*	+0.9*	-	-	4.17*	2.4*	-	-	2.11*	1.8*
Total leaf area (m^2/m^2)	-	-	−2.07*	−53.3*	-	-	−0.38*	−16.7*	-	-	0.14*	10.2*

Note. We represent the statistical significance of two comparisons, between simulations with different g_{1M} (*), and between the two model configurations (bold). A star (*) indicates low minus default g_{1M} responses pass a test for statistical significance, where the null hypothesis is that there is no difference between the low g_{1M} and default g_{1M} simulations. *Bolded* values indicate where the differences between the Land-Only-Fixed-Leaf (LndOnly) and Land-Atmosphere (LndAtm) configurations for low minus default g_{1M} pass a test for statistical significance, where the null hypothesis tested is that there is no difference between these two sets of differences.

decrease photosynthesis while an increase in VPD alone drastically decreased photosynthesis. Thus, we attribute the increase in VPD as the cause of the decrease in photosynthesis in both the Amazon and central NA because the magnitude of photosynthetic response to VPD alone was similar to the change in photosynthesis that we found between LndOnly and LndAtm (Figures 4b and 4d). In boreal Canada photosynthesis increases in response to elevated temperature alone and decreases in response to elevated VPD alone (Figure 4f). However, even though the direction of change in photosynthesis is consistent with the higher temperatures in LndAtm, the magnitude attributable to higher temperatures is much smaller in boreal Canada relative to magnitude attributable to either temperature or VPD in the other regions that we analyzed.

3.3. Elevated Atmospheric CO$_2$

Under elevated CO$_2$, we find that photosynthesis increases across the globe for all g_{1M} (water cost) simulations (Figures 5a–5c), with an increase in response to a doubling of preindustrial CO$_2$ of 66 PgC/year for default g_{1M}, 70 PgC/year for low g_{1M}, and 60 PgC/year for high g_{1M} (Figures 5a–5c, additional details of photosynthetic response to elevated CO$_2$ for the globe and the boreal, temperate, and tropical bands can be found in Table S2 in Supporting Information S1).

Generally we find that low g_{1M} increases photosynthesis further from default g_{1M}, and high g_{1M} perturbation moderates the increase in photosynthesis, although there are regions that do not follow this pattern (Figures 5d and 5e). However, overall, the additional photosynthetic response to g_{1M} perturbations are small relative to the photosynthetic response to elevated CO$_2$. Even so, assumptions about stomatal function modify the total global photosynthetic response to a doubling of preindustrial CO$_2$ by +6.4% for low g_{1M} and by −9.6% for high g_{1M} relative to default g_{1M}. At lower g_{1M}, photosynthesis increases relative to default g_{1M} in 58% of grid cells and decreases in 42% of grid cells. The change at higher g_{1M} is more spatially widespread, with increases relative to default g_{1M} in photosynthesis in only 27% of grid cells and decreases in 74% of grid cells.

We note that Australia has an absolute decrease in photosynthesis in response to elevated CO$_2$ with lower g_{1M} contrary to the rest of the globe, and a larger relative change in response to g_{1M} (Figure 5). We find that this can be explained by the substantial reduction in leaf area in response to lower g_{1M} (whether due to perturbations in g_{1M} or
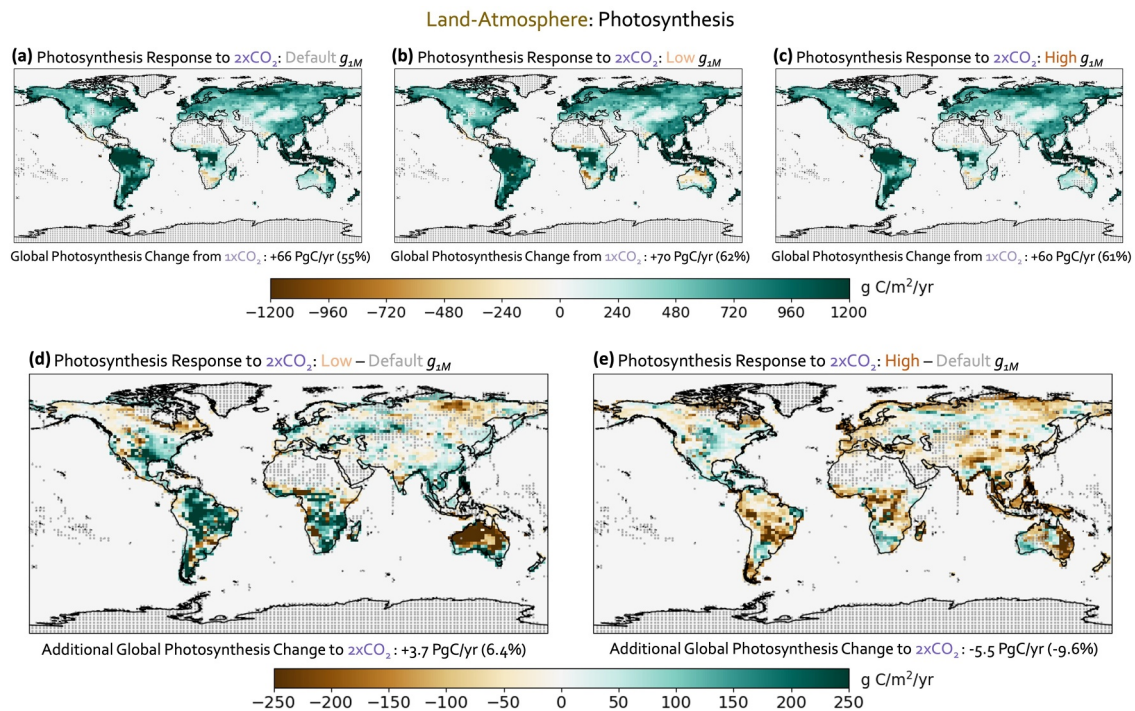
Figure 5. Photosynthesis difference spatial plots of default g_{1M} (water cost) between $1xCO_2$ and $2x$ preindustrial atmospheric CO_2 concentrations for (a) default, (b) low, and (c) high g_{1M} perturbations, where g_{1M} is constant for each comparison. Spatial difference plots showing the additional change in photosynthesis in response to a doubling of atmospheric CO_2 in the Land-Atmosphere (LndAtm) configuration when the default g_{1M} is replaced by (d) low g_{1M} and (e) high g_{1M} (see Section 2.3.3 for comparison details). The additional change in photosynthesis is calculated by taking the difference of the photosynthetic response to g_{1M} perturbation at $2xCO_2$ and $1xCO_2$ (e.g., $2xCO_2(low - default\ g_{1M}) - 1xCO_2(low - default\ g_{1M})$). Note the different scale in (a–e). Stippled grid cells represent differences that are not statistically significant. Grid cells are statistically significant if the photosynthetic response to g_{1M} perturbation at $2xCO_2$ is different from the photosynthetic response to g_{1M} perturbation at $1xCO_2$. Statistical methods are detailed in Section 2.5.

elevated CO_2), with leaf area nearly reaching zero in the west and halving in the east with lower g_{1M} (see further discussion of leaf area decrease in Text S2 and Figure S6 in Supporting Information S1).

4. Discussion

4.1. Inclusion of a Dynamic Atmosphere Evoked Strong Temperature and VPD Responses That Affected Photosynthesis

Broadly, we expected photosynthesis to decrease with lower g_{1M} (lower water cost) as photosynthesis and stomatal conductance are tightly coupled, with both regulated by stomata and iteratively calculated in the model. Although we find some regions of decrease in photosynthesis we also find regions of increase (Figures 3c and 3d). Not only was photosynthetic response to lower g_{1M} not consistent across regions, it was also not consistent across configurations of CESM2, flipping sign between increasing and decreasing photosynthetic response to the same change in g_{1M} depending on the inclusion of a dynamic atmosphere and prognostic leaf area (Figure 3e). The change in the sign of photosynthetic response to g_{1M} can be largely attributed to the inclusion of a dynamic atmosphere rather than prognostic leaf area (cf. Figure 3e and Figure S5 in Supporting Information S1).

To explain why photosynthesis shows a different direction of response to a decrease in g_{1M} when the atmosphere is allowed to dynamically respond (LndAtm compared to LndOnly), we explored four possible conjectures based on what we know about photosynthesis and its response to environmental factors. First, the low g_{1M} and default g_{1M} simulations could have differences in g_s in response to g_{1M} (conjecture 1; c1; Figure 6b). Second, photosynthesis could be responding to plant soil water stress (conjecture 2; c2; Figure 6c). Third, photosynthesis could be responding to a change in temperature which differs between LndAtm and LndOnly (conjecture 3; c3; Figure 6d). Fourth, photosynthesis could be responding to atmospheric water stress (conjecture 4; c4; Figure 6e). We note that given the coupled nature of the system, the four conjectures interact with each other (Figure 6a). To
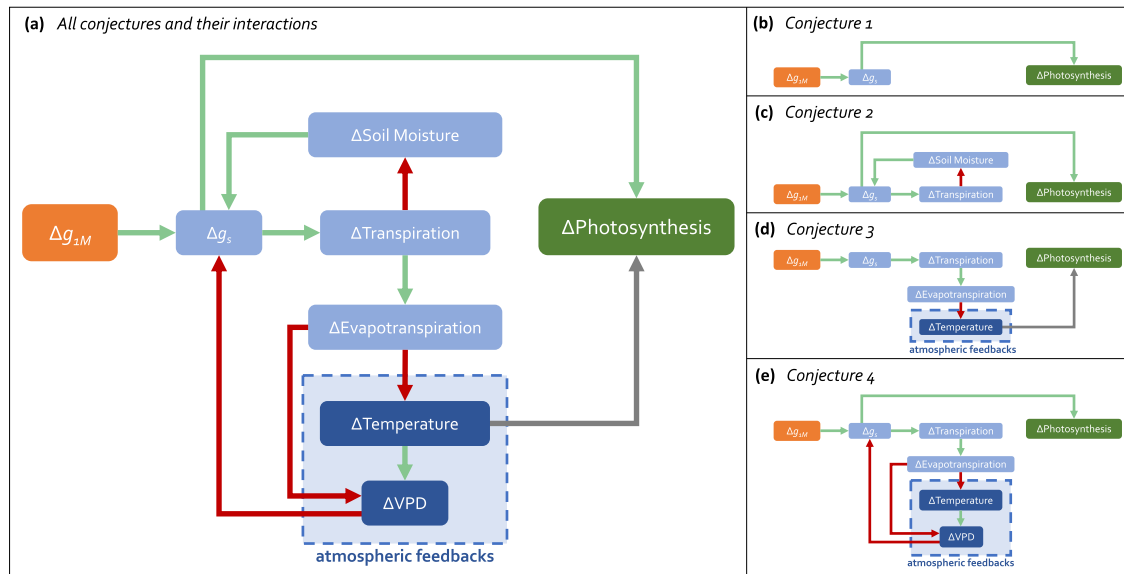
Figure 6. Flowcharts illustrating simplified conceptual diagrams of the conjectures of how g_{1M} perturbation impacts photosynthesis. (a) Shows all conjectures (c1–c4) and their interactions, while (b–d) focus on individual mechanisms: g_s (c1) in (b), soil moisture (c2) in (c), temperature (c3) in (d), and VPD (c4) in (e). Green arrows indicate positive relationships, red arrows negative relationships, and gray arrows relationships that depend on background climate. Changes in g_{1M} directly alter g_s which affects transpiration, sets off feedbacks through soil moisture (c2) and VPD (c4) that in turn influence g_s. Both g_s (c1) and temperature (c3) directly affect photosynthesis. Although leaf area is not shown in the diagram, changes in photosynthesis affect leaf area in prognostic leaf area simulations, which then directly feed back on to total photosynthesis and transpiration.

evaluate these conjectures we focus on regions that had a change in the sign of photosynthetic response to g_{1M} between the LndAtm and LndOnly low g_{1M} simulations (Figure 3e).

To start, there was a g_s decrease in response to lower g_{1M} perturbation in almost all regions for both the LndAtm and LndOnly simulations (Figures S3b and S4b in Supporting Information S1), which would on its own cause a decrease in photosynthesis, and thus changes in g_s (c1) alone cannot explain the difference in photosynthetic response between the two experimental groups (and hence model configurations). We note that the Tibetan Plateau region did not match the general global g_s response (Figures S3b and S4b in Supporting Information S1) because the C3 arctic grass PFT default g_{1M} used in CLM5 was lower than the low g_{1M} perturbation derived from Lin, Medlyn, Duursma, et al. (2015) (Figure 1a). The changes in soil water stress (c2), temperature (c3), and atmospheric water stress (c4) vary more across regions, so we discuss the response by region below.

4.1.1. VPD-Driven Photosynthesis Decreased in the Amazon and Central North America

For simulations with a prescribed atmosphere (LndOnly), we found a photosynthetic increase in the Amazon and central NA in response to lower g_{1M} (lower water cost) which is most likely driven by a reduction in soil water stress (c2) because temperature (c3) and VPD (c4) did not change much with fixed atmospheric forcing (Figure 4). During the Amazon dry season, the low g_{1M} simulation had similar g_s (c1) but lower soil water stress (c2) compared to the default g_{1M} simulation. This is due to a cumulative difference in transpiration rates allowing for soil water conservation that carries over into the dry season resulting in increased photosynthesis (Figure S7 in Supporting Information S1). In central NA, photosynthesis increased during the growing season as reduced soil water stress (c2) outweighed the decrease in g_s (Figure S7 in Supporting Information S1).

For simulations with a dynamic atmosphere and prognostic leaf area (LndAtm), we find that photosynthesis decreases. This can not be explained by soil water stress (c2), which is alleviated with lower g_{1M} in the Amazon and remains neutral in central NA. It is important to note that in the original formulation from Medlyn et al. (2011), g_{1M} was intended to dynamically respond to soil water stress (c2) but is static according to PFT within CLM5 due to limitations in soil-plant-atmosphere continuum representation (G. B. Bonan et al., 2014), however CLM5 does include a dynamic hydraulic conductance which includes soil, root, stem, and leaf water potentials that could address some of the limitations (Kennedy et al., 2019). This limitation implies that our results may not fully account the effects of soil water stress (c2) on photosynthesis.

The main differences between the response to lower g_{1M} in LndAtm and LndOnly are in the surface temperature (c3) and VPD (c4) responses. Temperature (c3) increased significantly in both the regions, which could potentially push plants beyond their thermal optima for photosynthesis (Yamori et al., 2014; Figures S3e and S4e in Supporting Information S1). However, CLM5 includes a representation of photosynthetic acclimation (Lombardozzi et al., 2015) which reduces the negative impact of hot temperatures.

We attribute the photosynthetic decreases with a dynamic atmosphere primarily to a response to VPD (c4) as the magnitude of expected photosynthetic response to an increase in VPD alone explains the total signal (Figures 4b and 4d) and is substantially larger than the response to temperature (c3) alone. The photosynthesis decrease in the Amazon is larger than in central NA, suggesting that plants in the Amazon are more sensitive to an increase in VPD (c4). This is consistent with prior modeling work showing that photosynthesis declines at high temperatures in tropical forests are mostly due to VPD effects rather than direct temperature effects in the land component of CESM2 (CLM5) (Zarakas, Swann, et al., 2024). In addition to VPD impacts on photosynthesis, recent observational and experimental methods found that photosynthesis decline at higher temperature can also be attributed to biochemical responses such as increases in mitochondrial respiration and photorespiration, Rubisco deactivation, and decreases in electron transport (Crous et al., 2024; Scafaro et al., 2023). Most land models lack full representation of these biochemical responses, so the projected decreases in photosynthesis at low g_{1M} may be underestimated.

4.1.2. Temperature Increased Photosynthesis in Boreal Canada

For boreal Canada we find a decrease in photosynthesis in response to lower g_{1M} (low water cost) in simulations with a prescribed atmosphere (LndOnly). In the LndOnly low g_{1M} simulation, we find support for the first conjecture as the decrease in g_s (c1) in boreal Canada had a greater effect on photosynthetic response than the small increase in soil water availability (c2) (Figure 4e). When the atmosphere is allowed to respond to low g_{1M}, photosynthesis increased in boreal Canada. Soil water availability (c2), temperature (c3), and VPD (c4) all increase. If boreal plants were strongly influenced by higher VPD (c4) as they were in the Amazon and central NA, this would cause a decrease in photosynthesis. Yet photosynthesis increased, implying that plants were more sensitive to the direct effects of increases in temperature (c3) than in VPD (c4) and that temperatures remained primarily below rather than above thermal optimum (Figure 4f). Although our direct attribution of the response of photosynthesis to an increase in temperature is smaller than the total increase in photosynthesis that we find, this could be explained by increased leaf area which is not included in our perturbed meteorology simulations (Figure S4 in Supporting Information S1; Table 2).

The expected photosynthetic responses from temperature for all three regions suggest that the total effect of temperature (c3) on photosynthesis is influenced by the background climate. A low baseline temperature region, like boreal Canada, may have positive responses to temperature increases while a high baseline temperature region, like the Amazon and central NA, may have negative responses to temperature increases, through both direct temperature effects and effects of higher VPD, which are indirectly driven by elevated temperature.

4.2. Implications for Choice of g_{1M} in Earth System Models

In CESM2, each PFT is assigned a single g_{1M} value, a practice which is common across similar models (G. Bonan, 2019; Sabot et al., 2022). Given that plants in the real world exhibit variation in g_{1M} (Lin, Medlyn, Duursma, et al., 2015), our results provide insight as to how and where Earth system models may be over or underestimating photosynthesis due to variation in g_{1M} in both the mean-state and in response to elevated CO_2.

Our simulated global photosynthesis values fall within that range of 83–172 PgC/year across the ensemble of 16 dynamic global vegetation models in the "Trends and drivers of regional scale sources and sinks of carbon dioxide" (TRENDY) project (Jung et al., 2020). However, our range of 99–120 PgC/year across perturbed g_{1M} highlights the potential magnitude of the impact of uncertainty in this one single aspect of stomatal function on photosynthesis in a single model. The fact that the difference between the high and low g_{1M} values spans a smaller range than TRENDY models suggests many other factors also influence photosynthesis, however, we demonstrate that sensitivity to g_{1M} is substantial and is varies regionally.

Because g_s and photosynthesis are coupled at the leaf level (G. J. Collatz et al., 1991; Franks et al., 2017; Medlyn et al., 2011), our simplest expectation is that the two should change in the same direction. In response to higher

g_{1M} (higher water cost), g_s is expected to increase, and thus in our simplest framework, photosynthesis is also expected to increase. Although g_s increased as expected with higher g_{1M}, photosynthesis substantially decreased across the globe (Figures 3a and 3b) due to an increase in soil water stress. The resulting very low photosynthesis with higher g_{1M} suggests that the 95th percentile g_{1M} values are too high to produce reasonable photosynthesis in CESM2, which leads us to the hypothesis that they are not representative of plants generally (see further discussion below).

With lower g_{1M} (lower water cost), g_s is expected to decrease, and thus in our simplest framework photosynthesis is also expected to decrease. However, we found increases in photosynthesis in some regions and decreases in other regions (Sections 3.2.2 and 3.2.3; Figures 3c and 3d), driven by varying plant responses to hotter temperatures that depend on the background climate. In hot regions like the Amazon, higher temperatures decrease photosynthesis, while in cold regions like boreal Canada higher temperatures increase photosynthesis. Thus, depending on the region, photosynthesis of plants with lower g_{1M} than that currently assumed in CESM2 could be either over or underestimated (see further discussion below).

In our elevated CO_2 simulations, g_{1M} modulates the sensitivity of photosynthesis increases to CO_2 increases (Equation 1). We expect lower g_{1M} to increase sensitivity, enhancing the photosynthetic increase, and higher g_{1M} to reduce sensitivity, dampening the photosynthetic increase (Medlyn et al., 2011). Our simulations align with these expectations, suggesting that CESM2 may underestimate photosynthesis if g_{1M} is lower than assumed, and overestimate photosynthesis if g_{1M} is higher than assumed. This also has implications for the total land carbon sink under elevated CO_2, with lower g_{1M} tending to increase gross photosynthesis and land carbon sink, while higher g_{1M} would do the opposite and tend to decrease the land carbon sink, all else being equal. However, warmer temperatures can counteract increases in the land carbon sink by increasing plant respiration and ecosystem carbon loss. Additionally, a closely related version of CESM2 has been shown to overestimate leaf area, and thus photosynthesis, compared to satellite observations (Song et al., 2021). Therefore, we note the caveat that the photosynthesis increases in our elevated CO_2 simulations may also be overestimated.

Our results quantify the potential impacts of varying g_{1M} on photosynthesis and identify regions where g_{1M} drives the largest changes. Specifically, we highlight the tropics where perturbed g_{1M} results in significant and large decreases for photosynthesis compared to the default g_{1M} at preindustrial atmospheric CO_2 concentrations (cf. Figures 3b and 3d).

The LndAtm high g_{1M} simulation had substantial photosynthesis decreases in the tropics, where broadleaf evergreen trees are the only PFT. This PFT has a high g_{1M} perturbation that is double the default g_{1M} value, which is a larger perturbation compared to that of other PFTs (Figure 1). We expect that individual plants with such a high g_{1M} would likely be drought-tolerant and be able to withstand a higher water cost for carbon gain. However, our simulations contradict this expectation with large decreases in photosynthesis for higher g_{1M}, driven by soil water stress. We suggest that the high g_{1M} values for the broadleaf evergreen tropical PFT are not compatible with CESM2 and thus we hypothesize that the values are not representative of typical plants in these regions. The Amazon also has similarly large photosynthetic decreases in the LndAtm low g_{1M} simulation, primarily driven by VPD increases, as discussed in Section 4.1.1. However, we cannot disentangle the sensitivity of the photosynthetic response to g_{1M} and to atmospheric feedbacks with our simulations.

Models differ in parameterizations, such as whether plant water stress is jointly determined by soil moisture and VPD, which can influence both the sensitivity of photosynthesis to g_{1M} and the relative importance of different drivers (Trugman, 2022; Trugman et al., 2018; Zarakas, Swann, et al., 2024). Despite these differences, we expect that most models would show qualitatively similar photosynthesis responses to those we observed in CESM2, where increasing g_{1M} past a certain threshold leads to decreases in photosynthesis. This would occur because changes in plant water use alter surface fluxes (Franks et al., 2024), changing VPD and temperature, which in turn influence photosynthesis through plant water stress. The general mechanism of land-atmosphere feedbacks on water stress are broadly represented across models, although the details would differ. Thus we hypothesize that the overall behavior should be expected in many models, while the specific threshold for this response will depend on how water stress is parameterized in each model.

4.3. Implications for Tree-Ring Based Observations

Our stomatal function perturbations through g_{1M} influence both g_s and photosynthesis, leading to changes in iWUE. In our simulations, iWUE increased with lower g_{1M} due to a decrease in g_s, while it decreased with higher g_{1M} due to an increase in g_s and a decrease in photosynthesis (Figures S1–S4 in Supporting Information S1). If plants had higher or lower g_{1M} than what is currently assumed in CESM2, iWUE would be overestimated or underestimated, respectively. Because our findings relate changes in stomatal function to changes in stomatal conductance, photosynthesis, and iWUE in the context of a dynamic atmosphere, they can be used to help interpret tree-based isotopic observations (Adams et al., 2020; Saurer et al., 2014).

4.4. Model Limitations in Representing Decoupling of g_s and Photosynthesis Under High Heat Stress

Currently in CESM2, which uses the optimal stomatal conductance formulation (Medlyn et al., 2011), plants tend to decrease g_s under high temperatures and high VPD to reduce water loss through transpiration. However, some plant species have been observed to increase g_s under heat stress, presumably increasing transpiration for evaporative cooling to prevent thermal leaf death or as an unavoidable response to intense heat (Marchin et al., 2022). This plant response to high temperatures is currently not implemented in any Earth system models and decouples photosynthesis and g_s (Marchin et al., 2023). In the context of our results, our simulations could be underestimating plant transpiration under high temperatures and high VPD conditions, particularly for the low g_{1M} simulations. The greater water fluxes could lead to different atmospheric feedbacks, potentially dampening the response of temperature and VPD increases. Additionally, the representation of leaf temperature is challenging in models and remains an unsolved problem. Errors in the estimation of leaf temperature relative to air temperatures impacts energy and water fluxes which could also potentially impact atmospheric feedbacks (Hawkins et al., 2022; Jiang et al., 2019). These atmospheric feedback changes can consequently influence the photosynthetic response.

5. Conclusions and Implications

Our research focused on how altering stomatal function, which governs water-carbon trade offs, affects photosynthesis. Overall we found that the answer was more complicated than one might initially guess, but that the response of photosynthesis can be explained by considering sensitivity to temperature and water availability. In particular, a dynamic atmosphere enabled the sign of photosynthetic response to reverse for low g_{1M} perturbation in the tropics and high latitudes. Other studies corroborate that choice of g_{1M} in land-atmosphere coupled simulations impacts the atmosphere (e.g., clouds and precipitation), underscoring the role of dynamic feedbacks between vegetation and climate (Franks et al., 2024). Thus, understanding how interactions between the land and the atmosphere are altered by land surface parameterizations is an important part of the process for model development and improvement.

Perturbed parameter ensembles (PPEs) have been used to quantify the impact of land parameter uncertainty and guide model calibration (Dagon et al., 2020; Kennedy et al., 2025; McNeall et al., 2016). PPEs reveal that parameters driving the most uncertainty can vary based on region and climate scenario (e.g., present-day and elevated CO_2), highlighting a challenge of calibrating individual parameters within complex models (Kennedy et al., 2025). These PPE studies find that land parameter uncertainty can strongly impact land-to-atmosphere fluxes, however most land parameter PPEs have not included the effects of a dynamic atmosphere. Land parameter uncertainty has a substantial impact on the mean climate-state when the atmosphere is allowed to respond (Zarakas, Kennedy, et al., 2024). Our work underscores the need to evaluate the sensitivity to parameter perturbations in the context of a dynamic atmosphere. Only considering land parameter perturbations under prescribed atmospheric conditions risks generating opposite responses to those under dynamic atmospheric conditions as we have shown here.

Plants have a distribution of g_{1M} values (Lin, Medlyn, Duursma, et al., 2015). If this real-world distribution of g_{1M} is substantially different from the g_{1M} values embedded in Earth system models, we risk inaccurately modeling not only the mean-state photosynthesis but also its response to global change, particularly in the tropics. In this study we show that alternate representations of stomatal function, whether due to plant adaptation to climate change or land-use changes, can substantially alter modeled photosynthesis and its predicted responses to environmental change, including a hotter elevated CO_2 world. We do not attempt to suggest an optimal g_{1M} value,

but we emphasize that more accurately constraining g_{1M} is important for constraining regional carbon sink and that g_{1M} needs to be evaluated in the context of a coupled Earth system.

We recognize that g_{1M} can be represented in ways other than being assigned based on plant functional type. Franks et al. (2024) showed that mean annual precipitation based g_{1M} values in coupled CESM2 simulations can better match observations of photosynthesis derived with data products derived FLUXNET eddy covariance towers and satellite remote sensing (i.e., FLUXCOM). Additionally, using a soil-plant system model with the absence of atmospheric feedbacks, Y. Liu et al. (2021) showed that estimating g_{1M} with a model-data fusion method based on remote sensing data and assigning values by hydraulic functional type, rather than PFT, yields a better match with evapotranspiration observations from the microwave-based Atmosphere-Land Exchange Inverse (ALEXI) algorithm. However, observations are still limited for representing g_{1M} with more granularity at global scales. Thus, measurements of stomatal function across a diversity of plant types, background climates, and CO_2 environments, ideally on mature plants in field settings and not just seedlings in greenhouses or growth chambers, would enable the community to build models that incorporate variability of plant traits and to more effectively use perturbed parameter ensembles to better quantify uncertainty in photosynthesis.

In our simulations we perturbed g_{1M} to its observational extremes (5th and 95th percentiles). Future simulations using a variety of other g_{1M} values (e.g., 25th and 75th percentiles) and incorporating different atmospheric feedbacks, including VPD and temperature feedbacks, could provide further insights to the sensitivity of photosynthesis to more moderate variation in g_{1M} and how it can affect global photosynthesis.

Conflict of Interest

The authors declare no conflicts of interest relevant to this study.

Data Availability Statement

The original data for this study are all available. Data used to perturb the stomatal slope parameter can be found at Lin, Medlyn, and Duursma (2015). Model output from the g_{1M} (water cost) perturbation simulations are available the Dryad Digital Repository for this paper (https://doi.org/10.5061/dryad.c59zw3rj0; A. X. Liu et al., 2025). Model output from the perturbed meteorology simulations used in this paper is available in another Dryad Digital Repository (https://doi.org/10.5061/dryad.h44j0zpw1; Zarakas, Swann, & Battisti, 2024). Code used for the analysis in this paper is available at A. Liu (2025). CESM2 is open source and all code can be found on Github at https://github.com/ESCOMP/CESM.

References

Adams, M. A., Buckley, T. N., & Turnbull, T. L. (2020). Diminishing CO_2-driven gains in water-use efficiency of global forests. *Nature Climate Change*, *10*(5), 466–471. https://doi.org/10.1038/s41558-020-0747-7

Arneth, A., Lloyd, J., Šantrucková, H., Bird, M., Grigoryev, S., Kalaschnikov, Y. N., et al. (2002). Response of central Siberian scots pine to soil water deficit and long-term trends in atmospheric CO_2 concentration. *Global Biogeochemical Cycles*, *16*. https://doi.org/10.1029/2000GB001374

Ball, J. T., Woodrow, I. E., & Berry, J. A. (1987). A model predicting stomatal conductance and its contribution to the control of photosynthesis under different environmental conditions. *Progress in Photosynthesis Research*, 221–224. https://doi.org/10.1007/978-94-017-0519-6_48

Bogenschutz, P. A., Gettelman, A., Hannay, C., Larson, V. E., Neale, R. B., Craig, C., & Chen, C. C. (2018). The path to CAM6: Coupled simulations with CAM5.4 and CAM5.5. *Geoscientific Model Development*, *11*(1), 235–255. https://doi.org/10.5194/GMD-11-235-2018

Bonan, G. (2019). Climate change and terrestrial ecosystem modeling. *Climate Change and Terrestrial Ecosystem Modeling*, 1–438. https://doi.org/10.1017/9781107339217

Bonan, G. B. (2008). Forests and climate change: Forcings, feedbacks, and the climate benefits of forests. *Science*, *320*(5882), 1444–1449. https://doi.org/10.1126/science.1155121

Bonan, G. B., Williams, M., Fisher, R. A., & Oleson, K. W. (2014). Modeling stomatal conductance in the earth system: Linking leaf water-use efficiency and water transport along the soil-plant-atmosphere continuum. *Geoscientific Model Development*, *7*(5), 2193–2222. https://doi.org/10.5194/gmd-7-2193-2014

Cheng, Y., Huang, M., Zhu, B., Bisht, G., Zhou, T., Liu, Y., et al. (2021). Validation of the community land model version 5 over the contiguous United States (CONUS) using in situ and remote sensing data sets. *Journal of Geophysical Research: Atmospheres*, *126*, e2020JD033539. https://doi.org/10.1029/2020JD033539

Collatz, G., Ribas-Carbo, M., & Berry, J. (1992). Coupled photosynthesis-stomatal conductance model for leaves of C4 plants. *Functional Plant Biology*, *19*(5), 519–538. https://doi.org/10.1071/PP9920519

Collatz, G. J., Ball, J. T., Grivet, C., & Berry, J. A. (1991). Physiological and environmental regulation of stomatal conductance, photosynthesis and transpiration: A model that includes a laminar boundary layer. *Agricultural and Forest Meteorology*, *54*(2–4), 107–136. https://doi.org/10.1016/0168-1923(91)90002-8

Cowan, I., & Farquhar, G. (1977). *Stomatal function in relation to leaf metabolism and environment* (pp. 471–505). Symposia of the Society for Experimental Biology. Retrieved from https://www.researchgate.net/publication/22384954_Stomatal_function_in_relation_to_leaf_metabolism_and_environment_Stomatal_function_in_the_regulation_of_gas_exchange

Crous, K. Y., Middleby, K. B., Cheesman, A. W., Bouet, A. Y., Schiffer, M., Liddell, M. J., et al. (2024). Leaf warming in the canopy of mature tropical trees reduced photosynthesis due to downregulation of photosynthetic capacity and reduced stomatal conductance. *New Phytologist*, *245*(4), 1421–1436. https://doi.org/10.1111/NPH.20320

Dagon, K., Sanderson, B. M., Fisher, R. A., & Lawrence, D. M. (2020). A machine learning approach to emulation and biophysical parameter estimation with the community land model, version 5. *Advances in Statistical Climatology, Meteorology and Oceanography*, *6*(2), 223–244. https://doi.org/10.5194/ascmo-6-223-2020

Danabasoglu, G., & Gent, P. R. (2009). Equilibrium climate sensitivity: Is it accurate to use a slab ocean model? *Journal of Climate*, *22*(9), 2494–2499. https://doi.org/10.1175/2008JCLI2596.1

Danabasoglu, G., Lamarque, J.-F., Bacmeister, J., Bailey, D. A., DuVivier, A. K., Edwards, J., et al. (2020). The Community Earth System Model Version 2 (CESM2). *Journal of Advances in Modeling Earth Systems*, *12*(2), e2019MS001916. https://doi.org/10.1029/2019MS001916

De Kauwe, M. G., Kala, J., Lin, Y. S., Pitman, A. J., Medlyn, B. E., Duursma, R. A., et al. (2015). A test of an optimal stomatal conductance scheme within the cable land surface model. *Geoscientific Model Development*, *8*(2), 431–452. https://doi.org/10.5194/GMD-8-431-2015

De Kauwe, M. G., Medlyn, B. E., Pitman, A. J., Drake, J. E., Ukkola, A., Griebel, A., et al. (2019). Examining the evidence for decoupling between photosynthesis and transpiration during heat extremes. *Biogeosciences*, *16*(4), 903–916. https://doi.org/10.5194/bg-16-903-2019

Farquhar, G. D., Caemmerer, S. V., & Berry, J. A. (1980). A biochemical model of photosynthetic CO_2 assimilation in leaves of C3 species. *Planta*, *149*(1), 78–90. https://doi.org/10.1007/bf00386231

Field, C. B., Jackson, R. B., & Mooney, H. A. (1995). Stomatal responses to increased CO_2: Implications from the plant to the global scale. *Plant, Cell and Environment*, *18*(10), 1214–1225. https://doi.org/10.1111/J.1365-3040.1995.TB00630.X

Frank, D. C., Poulter, B., Saurer, M., Esper, J., Huntingford, C., Helle, G., et al. (2015). Water-use efficiency and transpiration across European forests during the Anthropocene. *Nature Climate Change*, *5*(6), 579–583. https://doi.org/10.1038/nclimate2614

Franks, P. J., Berry, J. A., Lombardozzi, D. L., & Bonan, G. B. (2017). Stomatal function across temporal and spatial scales: Deep-time trends, land-atmosphere coupling and global models. *Plant Physiology*, *174*(2), 583–602. https://doi.org/10.1104/pp.17.00287

Franks, P. J., Herold, N., Bonan, G. B., Oleson, K. W., Dukes, J. S., Huber, M., et al. (2024). Land surface conductance linked to precipitation: Co-evolution of vegetation and climate in earth system models. *Global Change Biology*, *30*, e17188. https://doi.org/10.1111/GCB.17188

Hawkins, L. R., Bassouni, M., Anderegg, W. R., Venturas, M. D., Good, S. P., Kwon, H. J., et al. (2022). Comparing model representations of physiological limits on transpiration at a semi-arid ponderosa pine site. *Journal of Advances in Modeling Earth Systems*, *14*(11), e2021MS002927. https://doi.org/10.1029/2021MS002927

Jiang, Y., Kim, J. B., Trugman, A. T., Kim, Y., & Still, C. J. (2019). Linking tree physiological constraints with predictions of carbon and water fluxes at an old-growth coniferous forest. *Ecosphere*, *10*(4), e02692. https://doi.org/10.1002/ECS2.2692

Jung, M., Schwalm, C., Migliavacca, M., Walther, S., Camps-Valls, G., Koirala, S., et al. (2020). Scaling carbon fluxes from eddy covariance sites to globe: Synthesis and evaluation of the fluxcom approach. *Biogeosciences*, *17*(5), 1343–1365. https://doi.org/10.5194/BG-17-1343-2020

Keenan, T. F., Hollinger, D. Y., Bohrer, G., Dragoni, D., Munger, J. W., Schmid, H. P., & Richardson, A. D. (2013). Increase in forest water-use efficiency as atmospheric carbon dioxide concentrations rise. *Nature*, *499*(7458), 324–327. https://doi.org/10.1038/NATURE12291

Kennedy, D., Dagon, K., Lawrence, D. M., Fisher, R. A., Sanderson, B. M., Collier, N., et al. (2025). One-at-a-time parameter perturbation ensemble of the community land model, version 5.1. *Journal of Advances in Modeling Earth Systems*, *17*(8), e2024MS004715. https://doi.org/10.1029/2024MS004715

Kennedy, D., Swenson, S., Oleson, K. W., Lawrence, D. M., Fisher, R., da Costa, A. C. L., & Gentine, P. (2019). Implementing plant hydraulics in the community land model, version 5. *Journal of Advances in Modeling Earth Systems*, *11*, 485–513. https://doi.org/10.1029/2018MS001500

Knauer, J., Werner, C., & Zaehle, S. (2015). Evaluating stomatal models and their atmospheric drought response in a land surface scheme: A multibiome analysis. *Journal of Geophysical Research: Biogeosciences*, *120*(10), 1894–1911. https://doi.org/10.1002/2015JG003114

Kooperman, G. J., Chen, Y., Hoffman, F. M., Koven, C. D., Lindsay, K., Pritchard, M. S., et al. (2018). Forest response to rising CO_2 drives zonally asymmetric rainfall change over tropical land. *Nature Climate Change*, *8*(5), 434–440. https://doi.org/10.1038/s41558-018-0144-7

Laguë, M. M., Quetin, G. R., & Boos, W. R. (2023). Reduced terrestrial evaporation increases atmospheric water vapor by generating cloud feedbacks. *Environmental Research Letters*, *18*(7), 074021. https://doi.org/10.1088/1748-9326/ACDBE1

Lawrence, D., Fisher, R., Koven, C., Oleson, K., Swenson, S., Vertenstein, M., et al. (2018). *Technical description of version 5.0 of the community land model (CLM) (Tech. Rep.)*. National Center for Atmospheric Research.

Lawrence, D. M., Fisher, R. A., Koven, C. D., Oleson, K. W., Swenson, S. C., Bonan, G., et al. (2019). The community land model version 5: Description of new features, benchmarking, and impact of forcing uncertainty. *Journal of Advances in Modeling Earth Systems*, *11*(12), 4245–4287. https://doi.org/10.1029/2018MS001583

Leuning, R. (1995). A critical appraisal of a combined stomatal-photosynthesis model for C3 plants. *Plant, Cell and Environment*, *18*(4), 339–355. https://doi.org/10.1111/J.1365-3040.1995.TB00370.X

Li, F., Xiao, J., Chen, J., Ballantyne, A., Jin, K., Li, B., et al. (2023). Global water use efficiency saturation due to increased vapor pressure deficit. *Science*, *381*(6658), 672–677. https://doi.org/10.1126/science.adf5041

Lin, Y.-S., Medlyn, B., & Duursma, R. (2015). Optimal stomatal behaviour around the world [Dataset]. https://doi.org/10.6084/m9.figshare.1304289.v2

Lin, Y.-S., Medlyn, B. E., Duursma, R. A., Prentice, I. C., Wang, H., Baig, S., et al. (2015). Optimal stomatal behaviour around the world. *Nature Climate Change*, *5*(5), 459–464. https://doi.org/10.1038/nclimate2550

Liu, A. (2025). Code from: Atmospheric feedbacks reverse the sensitivity of modeled photosynthesis to stomatal function. *Zenodo*. https://doi.org/10.5281/zenodo.15272404

Liu, A. X., Zarakas, C. M., & Swann, A. L. S. (2025). Data from: Atmospheric feedbacks reverse the sensitivity of modeled photosynthesis to stomatal function [Dataset]. *Dryad*. https://doi.org/10.5061/dryad.c59zw3rj0

Liu, Y., Holtzman, N. M., & Konings, A. G. (2021). Global ecosystem-scale plant hydraulic traits retrieved using model-data fusion. *Hydrology and Earth System Sciences*, *25*(5), 2399–2417. https://doi.org/10.5194/hess-25-2399-2021

Lombardozzi, D. L., Bonan, G. B., Smith, N. G., Dukes, J. S., & Fisher, R. A. (2015). Temperature acclimation of photosynthesis and respiration: A key uncertainty in the carbon cycle-climate feedback. *Geophysical Research Letters*, *42*(20), 8624–8631. https://doi.org/10.1002/2015GL065934

Marchin, R. M., Backes, D., Ossola, A., Leishman, M. R., Tjoelker, M. G., & Ellsworth, D. S. (2022). Extreme heat increases stomatal conductance and drought-induced mortality risk in vulnerable plant species. *Global Change Biology*, *28*(3), 1133–1146. https://doi.org/10.1111/GCB.15976

Marchin, R. M., Medlyn, B. E., Tjoelker, M. G., & Ellsworth, D. S. (2023). Decoupling between stomatal conductance and photosynthesis occurs under extreme heat in broadleaf tree species regardless of water access. *Global Change Biology*, *29*(22), 6319–6335. https://doi.org/10.1111/GCB.16929

McNeall, D., Williams, J., Booth, B., Betts, R., Challenor, P., Wiltshire, A., & Sexton, D. (2016). The impact of structural error on parameter constraint in a climate model. *Earth System Dynamics*, *7*(4), 917–935. https://doi.org/10.5194/esd-7-917-2016

Medlyn, B. E., Duursma, R. A., Eamus, D., Ellsworth, D. S., Prentice, I. C., Barton, C. V., et al. (2011). Reconciling the optimal and empirical approaches to modelling stomatal conductance. *Global Change Biology*, *17*(6), 2134–2144. https://doi.org/10.1111/J.1365-2486.2010.02375.X

Medlyn, B. E., Kauwe, M. G. D., Lin, Y. S., Knauer, J., Duursma, R. A., Williams, C. A., et al. (2017). How do leaf and ecosystem measures of water-use efficiency compare? *New Phytologist*, *216*(3), 758–770. https://doi.org/10.1111/nph.14626

Sabot, M. E. B., De Kauwe, M. G., Pitman, A. J., Medlyn, B. E., Ellsworth, D. S., Martin-StPaul, N. K., et al. (2022). One stomatal model to rule them all? Toward improved representation of carbon and water exchange in global models. *Journal of Advances in Modeling Earth Systems*, *14*(4), e2021MS002761. https://doi.org/10.1029/2021MS002761

Saurer, M., Spahni, R., Frank, D. C., Joos, F., Leuenberger, M., Loader, N. J., et al. (2014). Spatial variability and temporal trends in water-use efficiency of European forests. *Global Change Biology*, *20*(12), 3700–3712. https://doi.org/10.1111/GCB.12717

Scafaro, A. P., Posch, B. C., Evans, J. R., Farquhar, G. D., & Atkin, O. K. (2023). Rubisco deactivation and chloroplast electron transport rates co-limit photosynthesis above optimal leaf temperature in terrestrial plants. *Nature Communications*, *14*(1), 1–10. https://doi.org/10.1038/s41467-023-38496-4

Song, X., Wang, D. Y., Li, F., & Zeng, X. D. (2021). Evaluating the performance of CMIP6 Earth system models in simulating global vegetation structure and distribution. *Advances in Climate Change Research*, *12*(4), 584–595. https://doi.org/10.1016/J.ACCRE.2021.06.008

Trugman, A. T. (2022). Integrating plant physiology and community ecology across scales through trait-based models to predict drought mortality. *New Phytologist*, *234*(1), 21–27. https://doi.org/10.1111/NPH.17821

Trugman, A. T., Medvigy, D., Mankin, J. S., & Anderegg, W. R. (2018). Soil moisture stress as a major driver of carbon cycle uncertainty. *Geophysical Research Letters*, *45*, 6495–6503. https://doi.org/10.1029/2018GL078131

Wilks, D. S. (2016). "The stippling shows statistically significant grid points": How research results are routinely overstated and overinterpreted, and what to do about it. *Bulletin of the American Meteorological Society*, *97*(12), 2263–2273. https://doi.org/10.1175/BAMS-D-15-00267.1

Wolz, K. J., Wertin, T. M., Abordo, M., Wang, D., & Leakey, A. D. (2017). Diversity in stomatal function is integral to modelling plant carbon and water fluxes. *Nature Ecology & Evolution*, *1*(9), 1292–1298. https://doi.org/10.1038/s41559-017-0238-z

Yamori, W., Hikosaka, K., & Way, D. A. (2014). Temperature response of photosynthesis in C3, C4, and CAM plants: Temperature acclimation and temperature adaptation. *Photosynthesis Research*, *119*(1–2), 101–117. https://doi.org/10.1007/s11120-013-9874-6

Zarakas, C. M., Kennedy, D., Dagon, K., Lawrence, D. M., Liu, A., Bonan, G., et al. (2024). Land processes can substantially impact the mean climate state. https://doi.org/10.31223/X50T2F

Zarakas, C. M., Swann, A. L. S., & Battisti, D. S. (2024). Synthetic meteorology model simulations [Dataset]. *Dryad*. https://doi.org/10.5061/dryad.h44j0zpw1

Zarakas, C. M., Swann, A. L. S., Koven, C. D., Smith, M. N., & Taylor, T. C. (2024). Different model assumptions about plant hydraulics and photosynthetic temperature acclimation yield diverging implications for tropical forest gross primary production under warming. *Global Change Biology*, *30*(9), e17449. https://doi.org/10.1111/GCB.17449